

# Suppressing Lithium Dendrite Formation by Slowing Its Desolvation Kinetics

*Huicong Yang<sup>1,2</sup>, Lichang Yin<sup>1,2</sup>, Huifa Sh<sup>3,4</sup>, Kuang He<sup>1,2</sup>, Hui-Ming Cheng<sup>1,2,5</sup> and  
Feng Li<sup>\*1,2</sup>*

<sup>1</sup>Shenyang National Laboratory for Materials Science, Institute of Metal Research,  
Chinese Academy of Science, Shenyang 110016, China, E-mail: [fli@imr.ac.cn](mailto:fli@imr.ac.cn)

<sup>2</sup>School of Materials Science and Engineering, University of Science and Technology  
of China, Shenyang 110016, China

<sup>3</sup>Engineering Laboratory for Functionalized Carbon Materials, Shenzhen Key  
Laboratory for Graphene-based Materials, Graduate School at Shenzhen, Tsinghua  
University, Shenzhen 518055, China

<sup>4</sup>Laboratory of Advanced Materials, School of Materials Science and Engineering,  
Tsinghua University, Beijing 100084, China

<sup>5</sup>Shenzhen Geim Graphene Center, Tsinghua-Berkeley Shenzhen Institute, Tsinghua  
University, Shenzhen 518055, China

\*Corresponding Author: [fli@imr.ac.cn](mailto:fli@imr.ac.cn) of Feng Li

**Chemicals.** 1, 2-dimethoxyethane (DME, 99.9%), 1, 3-dioxolane (DOL, 99.8%), tetraethylene glycol dimethyl ether (TEGDME, 99.0%) and lithium titanate (LTO, 98%) were purchased from Sigma-Aldrich. Lithium nitrate ( $\text{LiNO}_3$ , 99.99%) was purchased from Aladdin. Lithium bis(trifluoromethanesulfonyl)imide (LiTFSI, 99.8%) was purchased from Dodo Chem. All the chemicals were directly used without any further treatment or purification.

**Cathode preparation.** 80wt% LTO or LFP, 10wt% Ketjen Black and 10wt% PVDF (polyvinylidene Fluoride) were mixed together with NMP (N-methyl pyrrolidinone) to form a uniform slurry. The slurry was coated on aluminum foils and dried in a vacuum oven at 60 °C for 24 h. The foils were cut into circular cathodes with a diameter of 12 mm. The final loading of LTO was 2.9  $\text{mg cm}^{-2}$  and of LFP was 4.0  $\text{mg cm}^{-2}$ .

**Cell assembly.** Each test cell used a high purity lithium foil as the anode, Celgard 2500 as the separator, and a 60  $\mu\text{L}$  electrolyte dose. Different cathodes were used for the testing.

**Electrolyte preparation.** Electrolytes were prepared under an argon atmosphere in a glove box (<0.1 ppm of water and oxygen). The commonly used DME+DOL electrolyte was prepared by mixing 1 mol LiTFSI with 1 L DME+DOL mixed solvent (volume ratio 1:1). The DME+DOL+TEGDME electrolyte was prepared by adding 1

mol LiTFSI to 1 L mixed DME+DOL+TEGDME solvent (volume ratio 1:1:2). 2wt% LiNO<sub>3</sub> was added to the electrolytes where necessary.

**Material characterization.** Raman spectroscopy was obtained using a Horiba LabRAM HR800, excited by a 532 nm laser with a laser spot size of  $\sim 1 \mu\text{m}^2$  with a 50 $\times$  objective lens. The morphology of the samples was characterized using a SEM (FEI Nova Nano-SEM 430, 15 kV).

**Electrochemical testing.** Electrochemical impedance spectroscopy (EIS) was obtained on an electrochemical station (Biologic VSP-300). The tests were conducted at open circuit with an amplitude of 5 mV in the frequency range  $10^{-2}$  Hz to 100 kHz in a two-electrode system. Tafel plots and electrochemical stable window tests were obtained using linear sweep voltammetry (LSV) with a scan speed of 0.2 mV/s in a quasi-static process (This scan speed is widely accepted for obtaining a steady state for further current ( $i$ )-overpotential ( $\eta$ ) analysis). We choose LTO for the preliminary LSV test to avoid any possible effect of a solid electrolyte interface film in different electrolytes because the working voltage of LTO is above the reduction voltage of commonly used ether and ester electrolytes. Coulombic efficiency was tested using Li-Cu cells at a constant current density of  $1 \text{ mA cm}^{-2}$ , the electrodeposition time was 1 h and the cut-off voltage for the electrostripping process was 1 V. Samples for examining the lithium electrodeposition morphology on a Cu foil were prepared at current densities of  $1 \text{ mA cm}^{-2}$ ,  $3 \text{ mA cm}^{-2}$  and  $5 \text{ mA cm}^{-2}$ . All the samples had  $1 \text{ mAh cm}^{-2}$  lithium

electrodeposited. Symmetric cells were tested at a current density of  $1 \text{ mA cm}^{-2}$ , with a 1 h charge process and a 1 h discharge process, all the symmetric cells were pre charged for 2 h and then pre discharged for 4 h to clean the surface of lithium foils. Li | LFP full cells were assembled with LFP cathodes and a Cu foil with pre-electrodeposited lithium as anodes. The amount of pre-electrodeposited lithium was  $0.3 \text{ mAh cm}^{-2}$  at a current density of  $1 \text{ mA cm}^{-2}$ .

**DFT calculations methods.** Spin-polarized density functional theory (DFT) calculations were performed using the Vienna Ab-initio Simulation Package<sup>[1]</sup> with the projector-augmented wave (PAW) method.<sup>[2]</sup> The Perdew-Burke-Ernzerhof functional<sup>[3]</sup> and the PAW method were adopted to describe the exchange-correlation term and electron-ion interaction, respectively. The energy cutoff for plane-wave basis was set to 400 eV and a dipole correction was used for  $\text{Li}^+$ -involved systems. All DFT calculations were conducted under normal precision with a Gaussian smearing width of 0.05 eV. H (1s), Li (1s, 2s), C (2s, 2p), and O (2s, 2p) electrons were treated as valence states. Only the Gamma point was used to sample the Brillouin zone for all calculations, since a large supercell ( $30\text{\AA} \times 30\text{\AA} \times 20\text{\AA}$ ) was constructed to investigate the coordination between  $\text{Li}^+$  and different solvents involved in this work. The convergence criteria of  $1 \times 10^{-6}$  eV for total energy was used for structure relaxation. All atomic structures presented in this study were generated by using VESTA code.<sup>[4]</sup>

**Activation energy calculations by Rct-Temperature fitting.** First, the charge transfer

resistances of the cells with the DME+DOL or DME+DOL+TEGDME electrolyte were measured at 0 °C, 10 °C, 20 °C, 30 °C and 40 °C using an electrochemical station (Biologic VSP-300). The test was conducted at open circuit with an amplitude of 5 mV in the frequency range 10<sup>-1</sup> Hz to 100 kHz in a two-electrode system. Based on Equations (1), (2) and (3), the activation energy can be calculated.

$$i_0 = F A k^0 C_O^\alpha C_R^\beta \quad (1);$$

$$k^0 = Cons. \times e^{\frac{-\Delta G}{RT}} \quad (2);$$

$$R_{ct} = \frac{RT}{n F i_0} \quad (3);$$

Equation (1) says that the exchange current ( $i_0$ ) of this lithium electrostripping/deposition reaction is related to the concentration ( $C_O$  and  $C_R$ ), electrode surface area ( $A$ ) and reaction rate constant ( $k^0$ ) for the charge transfer reaction.  $F$  is Faraday's constant. Since the only difference in the two cell systems is the solvents, all the physical parameters should be the same except for  $k^0$ . In Equation (2),  $k^0$  is in the form of an Arrhenius Equation.  $\Delta G$  is the activation energy of the charge transfer reaction,  $R$  is the perfect gas constant and  $T$  is the temperature. Because the EIS measurement is a small polarization method, Equation (3) can be used to establish the relationship between  $R_{ct}$  (charge transfer resistance) and  $i_0$ . Through these three equations, Equation (4) can be deduced:

$$\ln\left(\frac{RT}{R_{ct}}\right) = -\Delta G \times \frac{1000}{RT} + Cons. \quad (4)$$

When plotting  $\frac{1000}{RT}$  as the x-coordinate and  $\ln\left(\frac{RT}{R_{ct}}\right)$  as the y-coordinate, the slops of the straight line gives  $-\Delta G$  (kJ mol<sup>-1</sup>). Following this method, the activation energies

of the lithium electrostripping/deposition reaction in the two electrolytes are obtained.

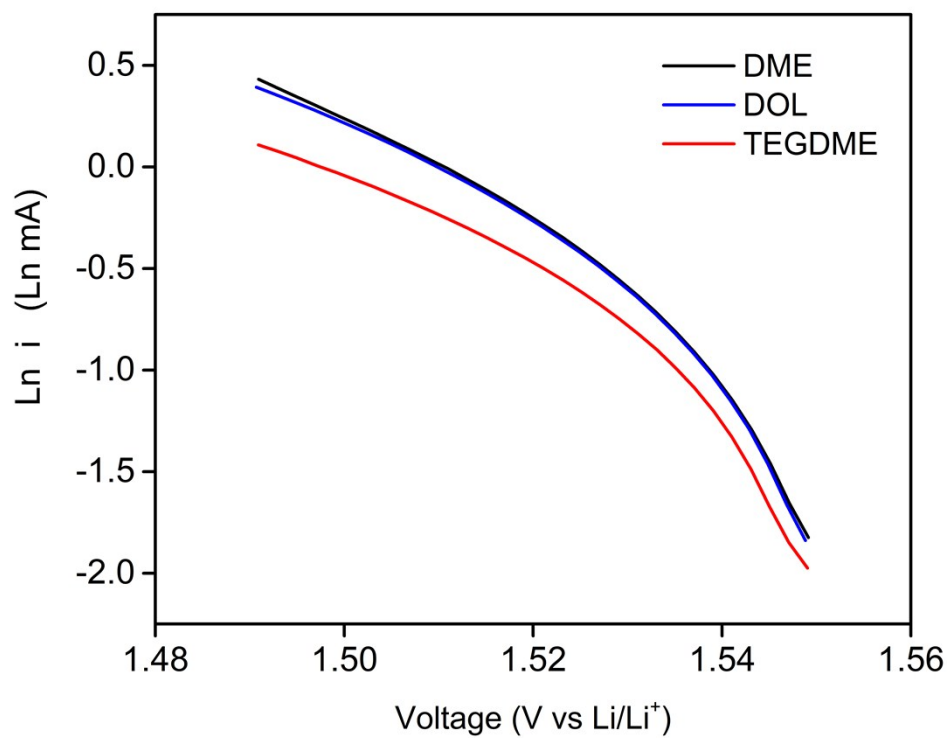


**Figure S1.** Tafel plots for different electrolytes with 1 M LiTFSI in 1 L DME, DOL or TEGDME.

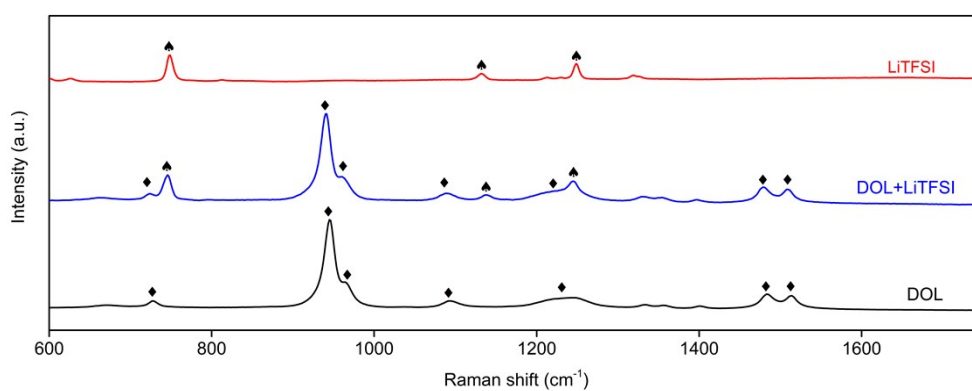


**Figure S2.** Raman spectrum of pure LiTFSI, pure DOL and 1 mol LiTFSI in 1 L DOL, where ♠ represents the Raman peaks in LiTFSI and ♦ represents the Raman peaks in DOL.

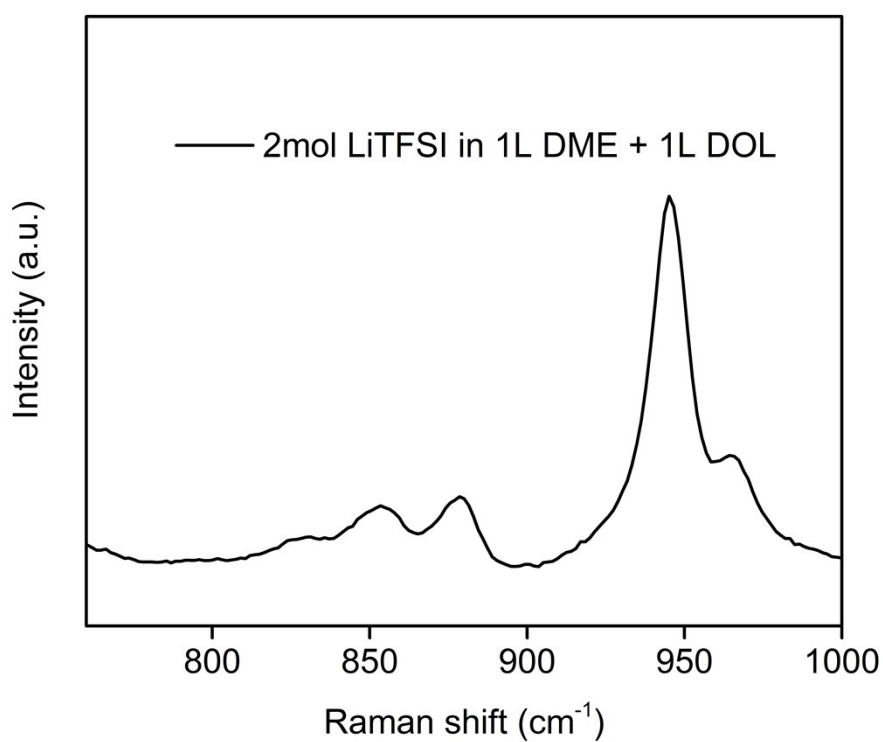


**Figure S3.** Raman spectrum of 2 mol LiTFSI in 1 L DME + 1 L DOL.

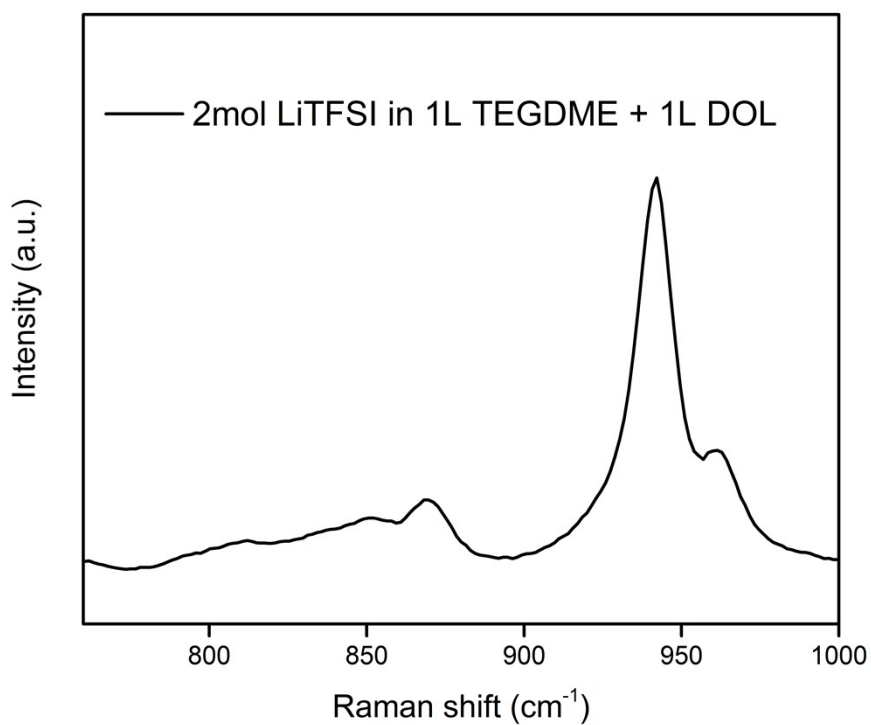


**Figure S4.** Raman spectrum of 2 mol LiTFSI in 1 L TEGDME + 1 L DOL.

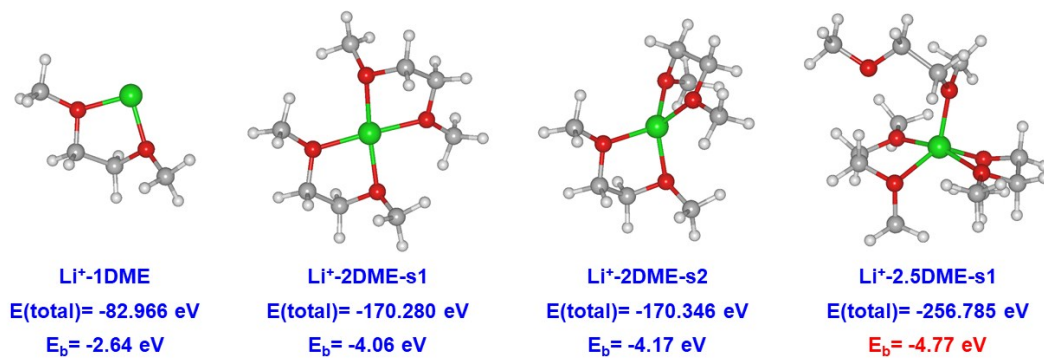


**Figure S5.** DFT calculations of Li<sup>+</sup>-DME coordination interactions. The white, grey, green and red balls represent hydrogen, carbon, lithium and oxygen atoms, respectively.

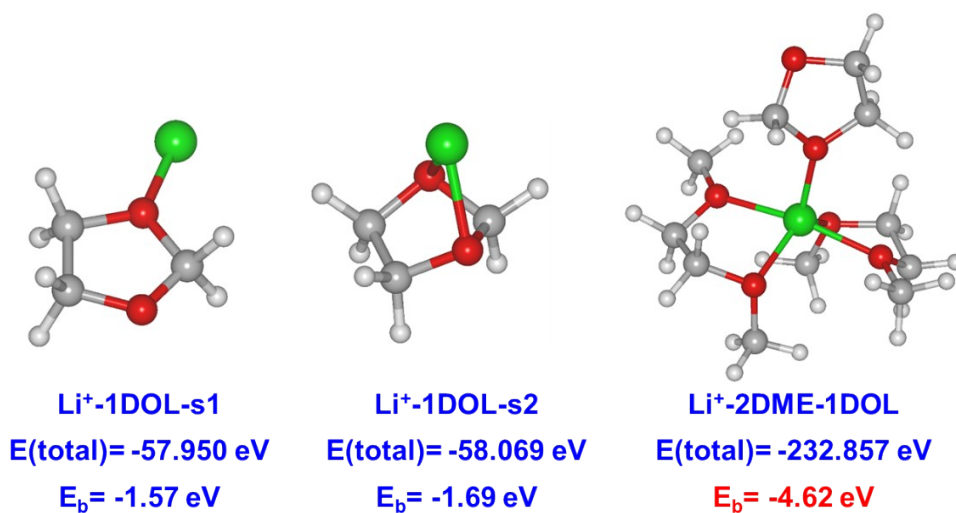


**Figure S6.** DFT calculations of Li<sup>+</sup>-DOL/DME coordination interactions.

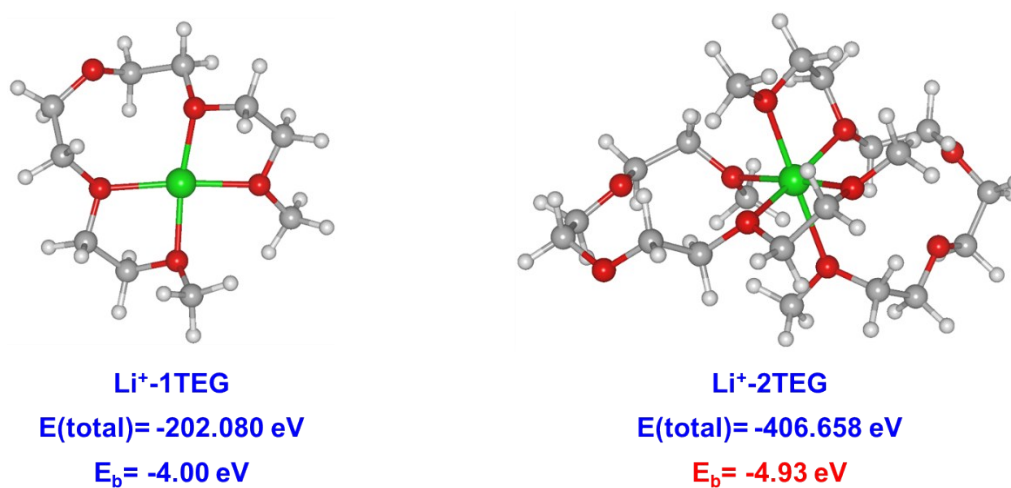


**Figure S7.** DFT calculations of Li<sup>+</sup>-TEGDME coordination interactions.

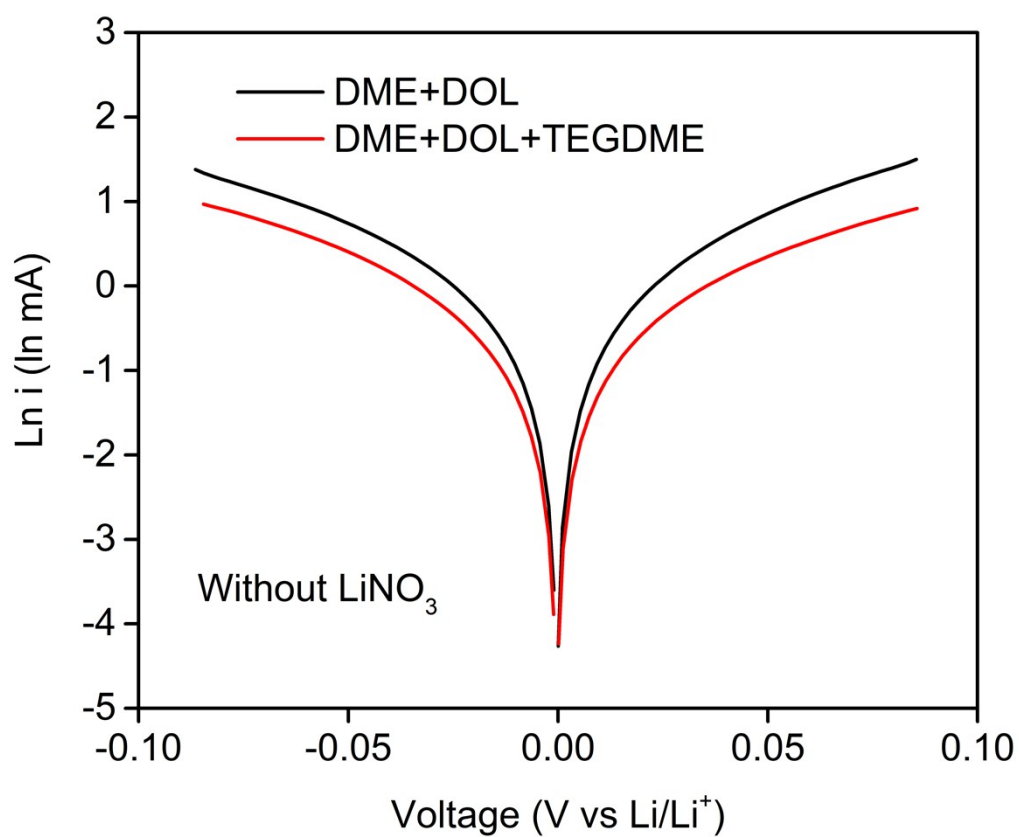


**Figure S8.** The Li | Li symmetric cell Tafel plot test of the DME+DOL+TEGDME and DME+DOL electrolytes without  $\text{LiNO}_3$ .

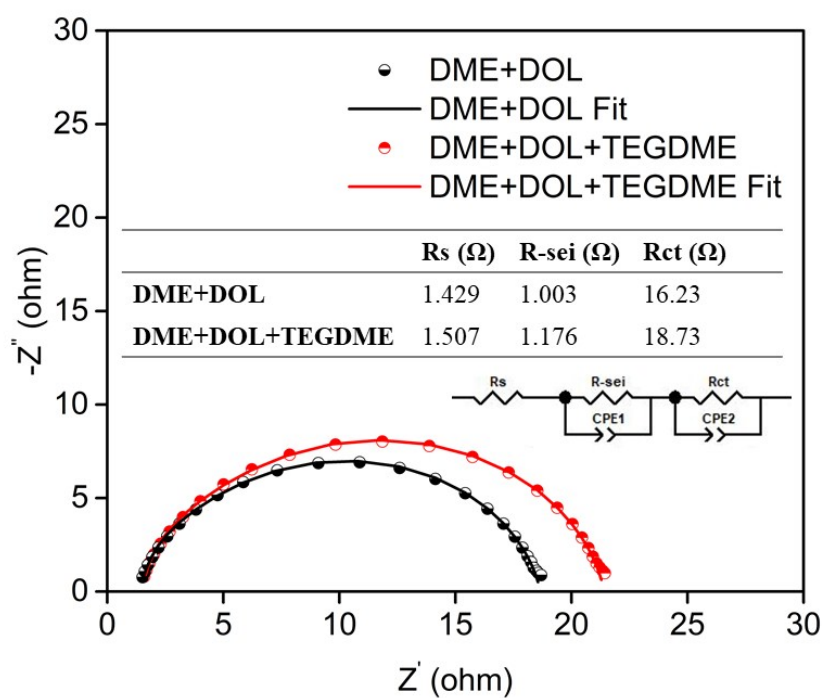


**Figure S9.** EIS of the cells with different electrolytes (with  $\text{LiNO}_3$ ).

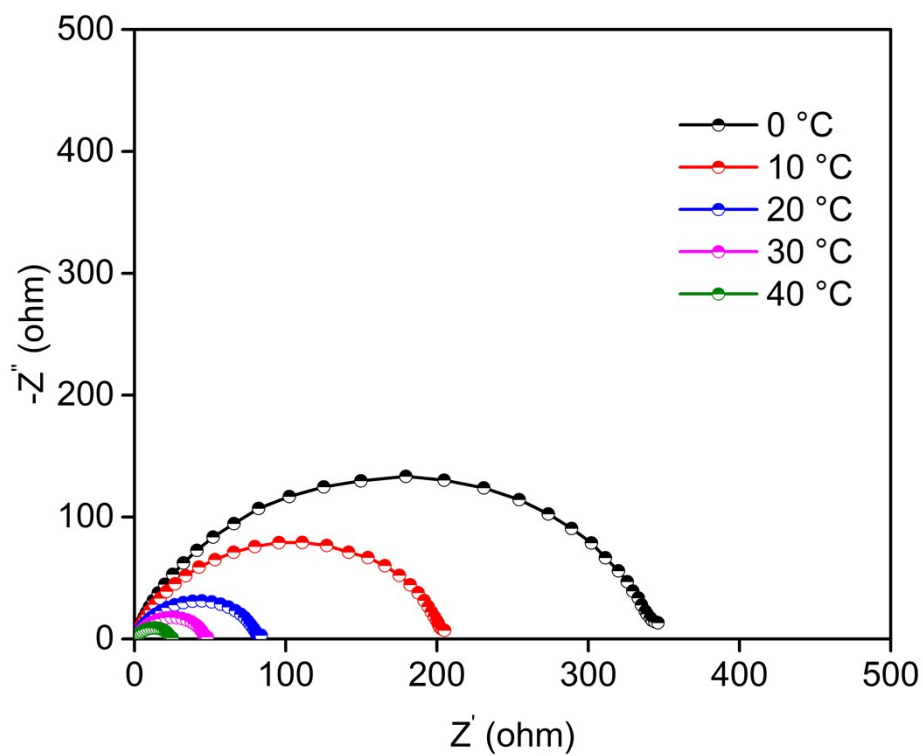


**Figure S10.** EIS of the cells with the DME+DOL electrolyte (without  $\text{LiNO}_3$ ) at

different temperatures.

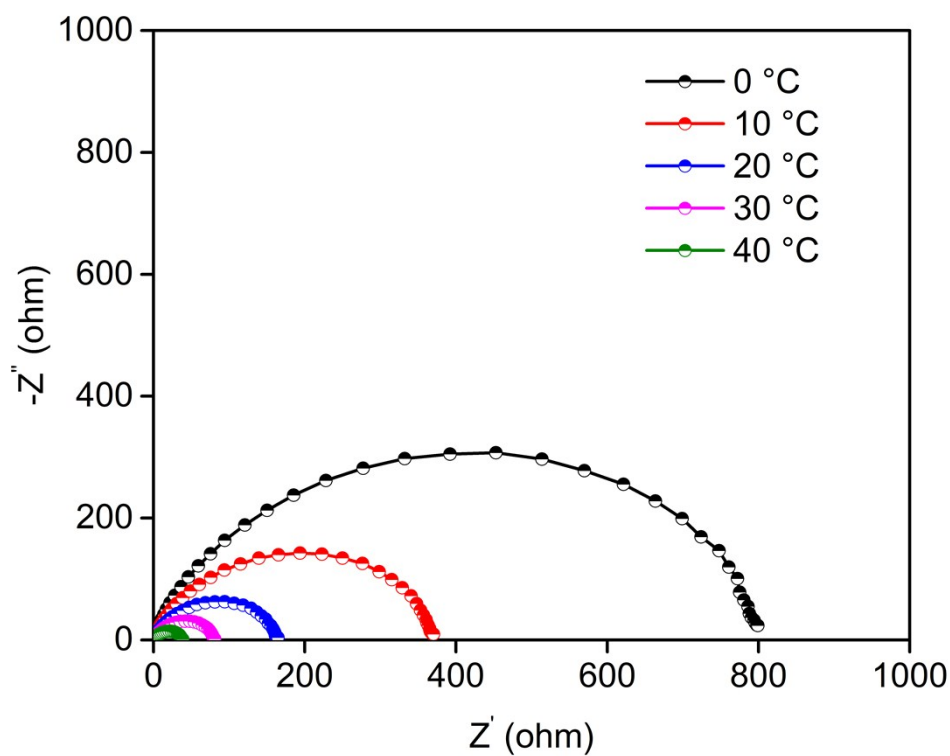


**Figure S11.** EIS of the cells with the DME+DOL+TEGDME electrolyte (without  $\text{LiNO}_3$ ) at different temperatures.

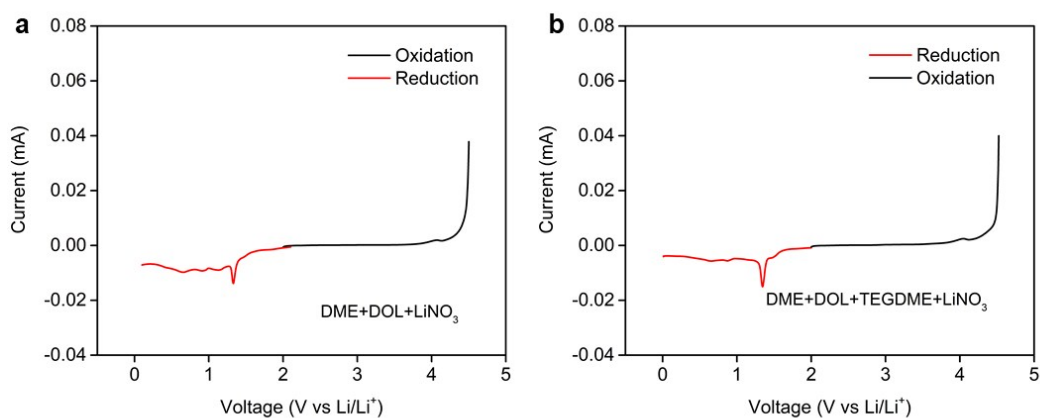


**Figure S12.** Electrochemical stable window tests of a) DME+DOL and b) DME+DOL+TEGDME electrolytes.

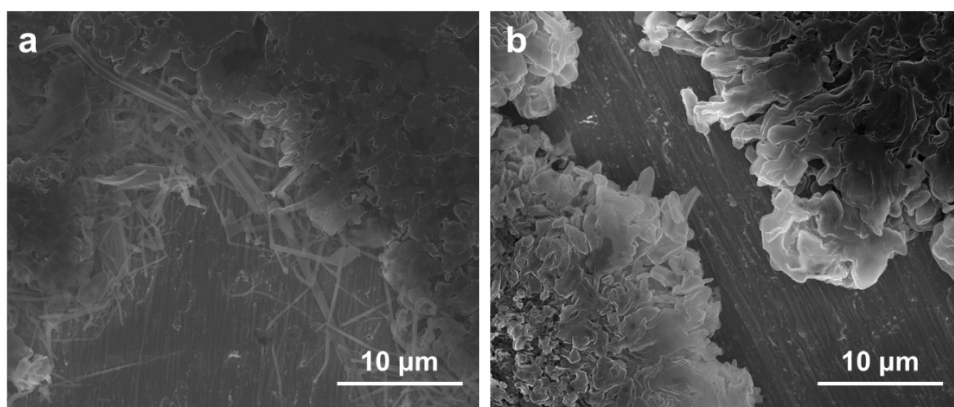


**Figure S13.** SEM images of the lithium electrodeposition morphology on a Cu foil in different electrolytes at  $1 \text{ mA cm}^{-2}$ : a) DME+DOL without  $\text{LiNO}_3$ ; b) DME+DOL+TEGDME without  $\text{LiNO}_3$ .

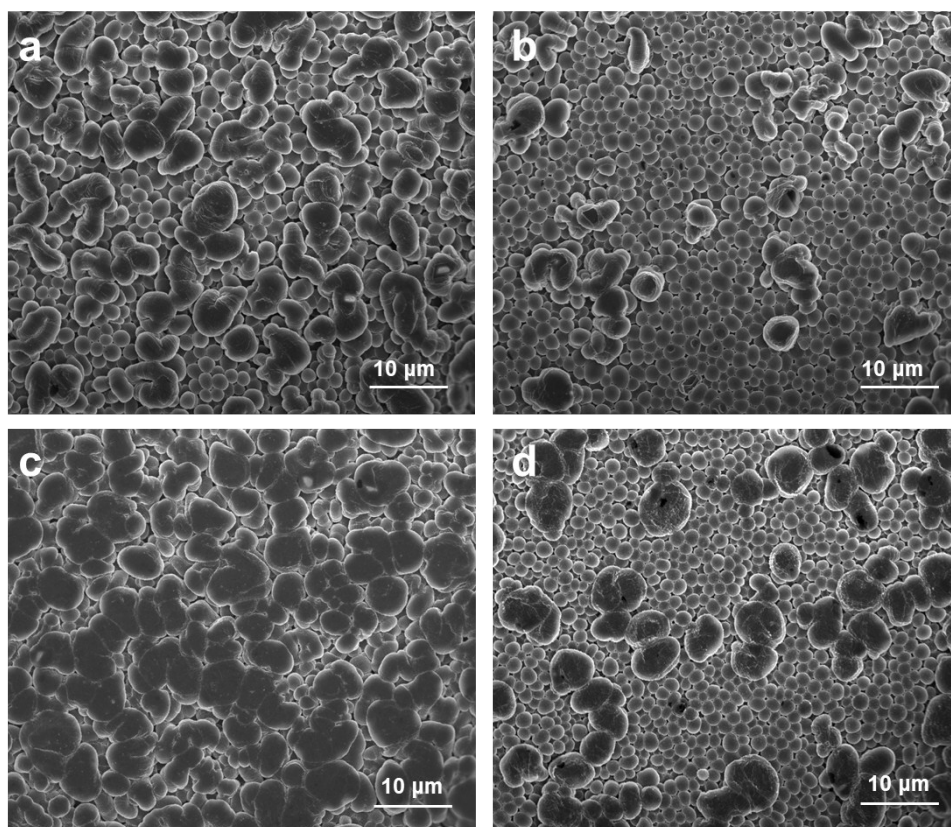


**Figure S14.** SEM images of lithium electrodeposition on Cu foils in different electrolytes at different current densities: a) DME+DOL electrolyte at  $3 \text{ mA cm}^{-2}$ ; b)

DME+DOL+TEGDME electrolyte at 3 mA cm<sup>-2</sup>; c) DME+DOL electrolyte at 5 mA cm<sup>-2</sup>; d) DME+DOL+TEGDME electrolyte at 5 mA cm<sup>-2</sup>.

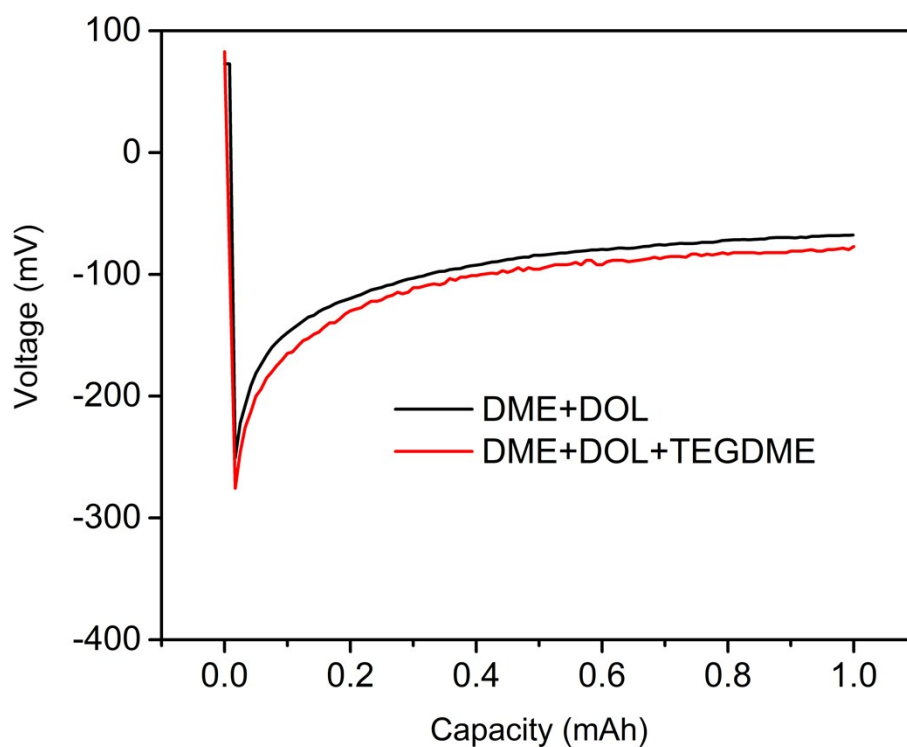


**Figure S15.** The initial lithium electrodeposition curves on a Cu foil at 3 mA cm<sup>-2</sup> in different electrolytes.

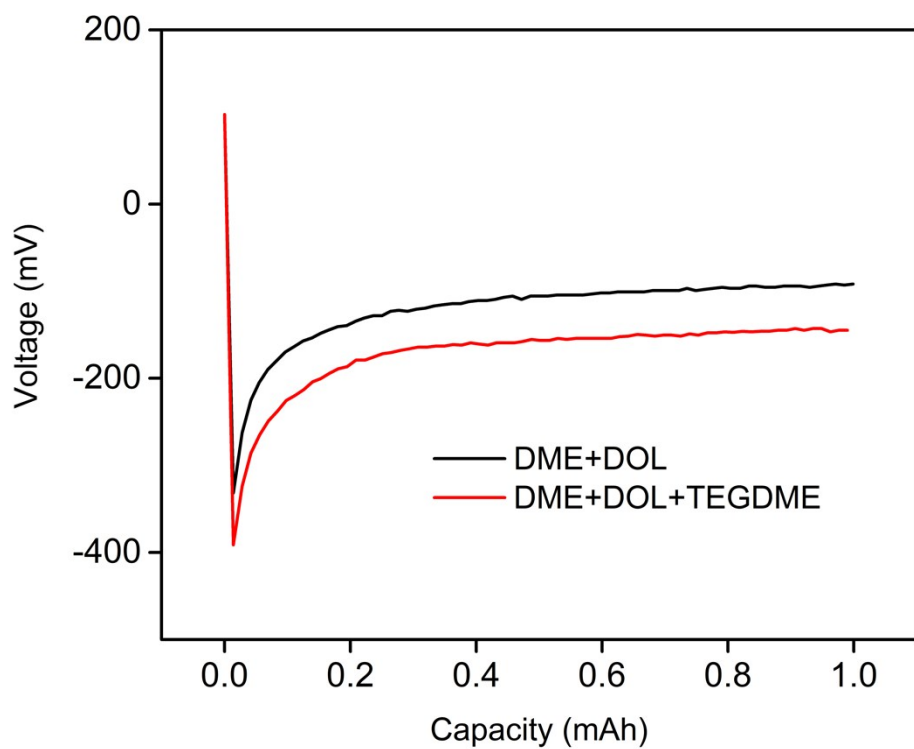


**Figure S16.** The initial lithium electrodeposition curves on a Cu foil at  $5 \text{ mA cm}^{-2}$  in different electrolytes.

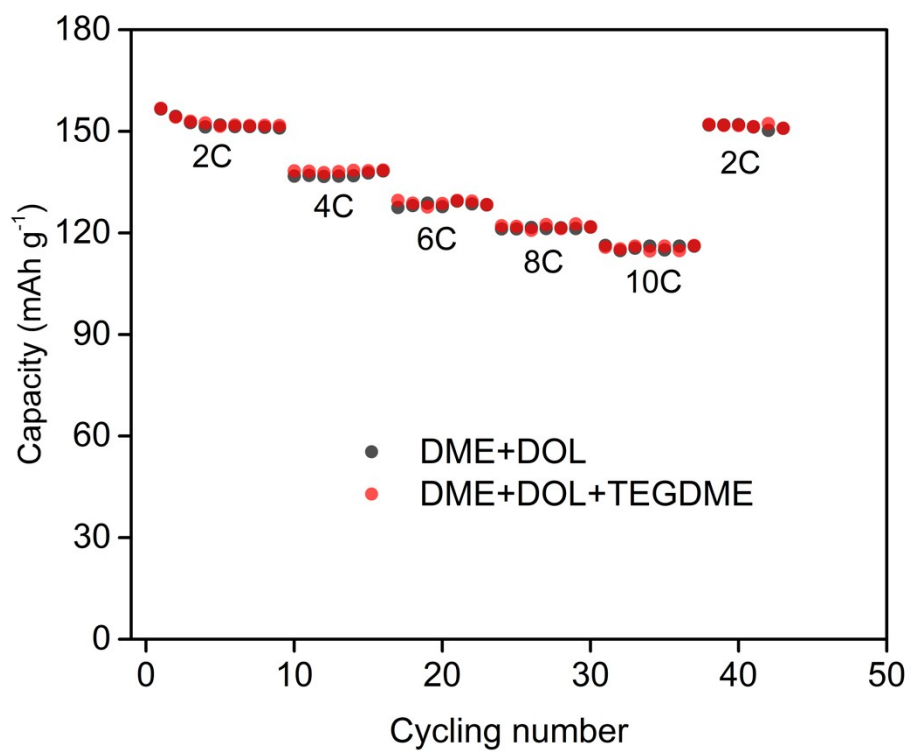


**Figure S17.** Rate performance of Li | LTO cells with different electrolytes.

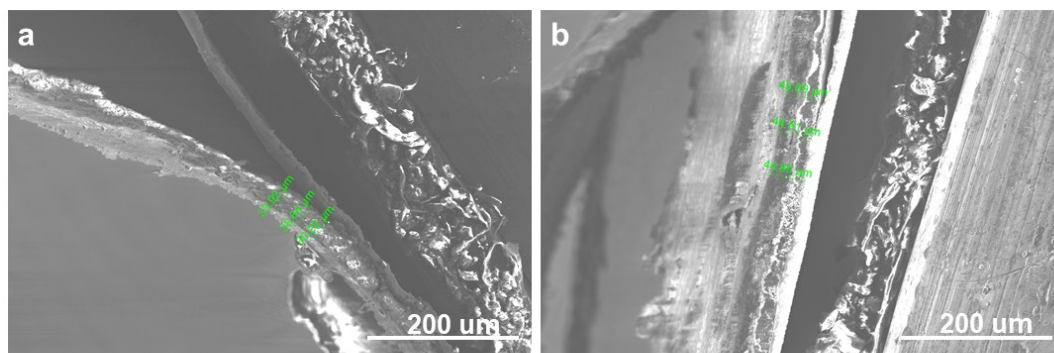


**Figure S18.** SEM images of SEI films on Cu foil in different electrolyte after 40 cycle's CE test: (a) SEI film formed in DDT electrolyte; (b) SEI film formed in DD electrolyte.

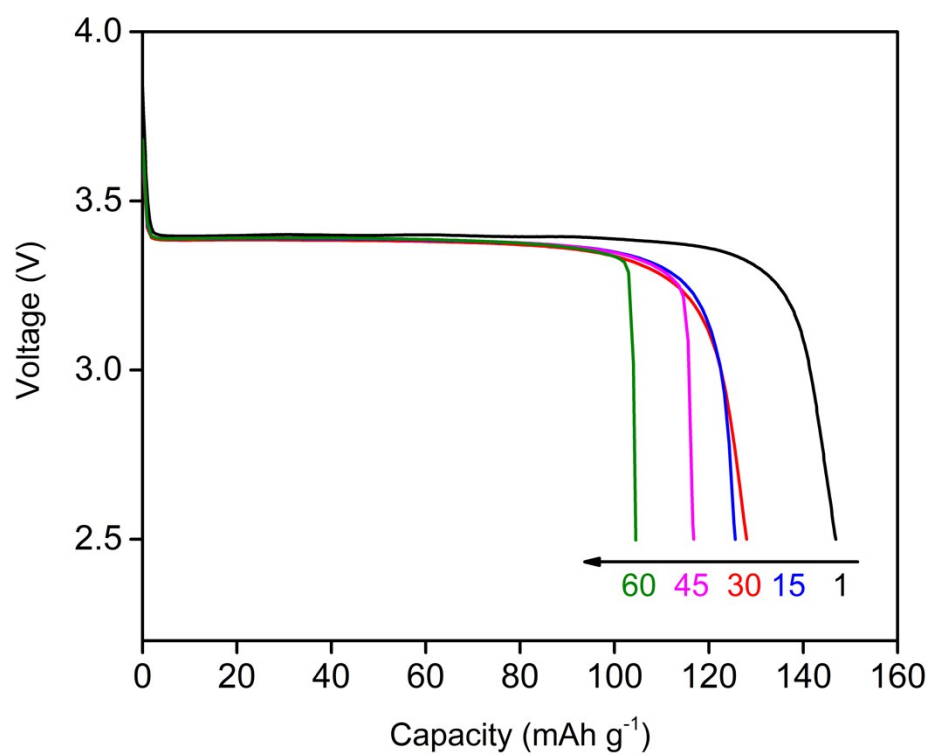


**Figure S19.** Discharge curves of a Li | LFP full cell with DME+DOL electrolyte at different cycles.

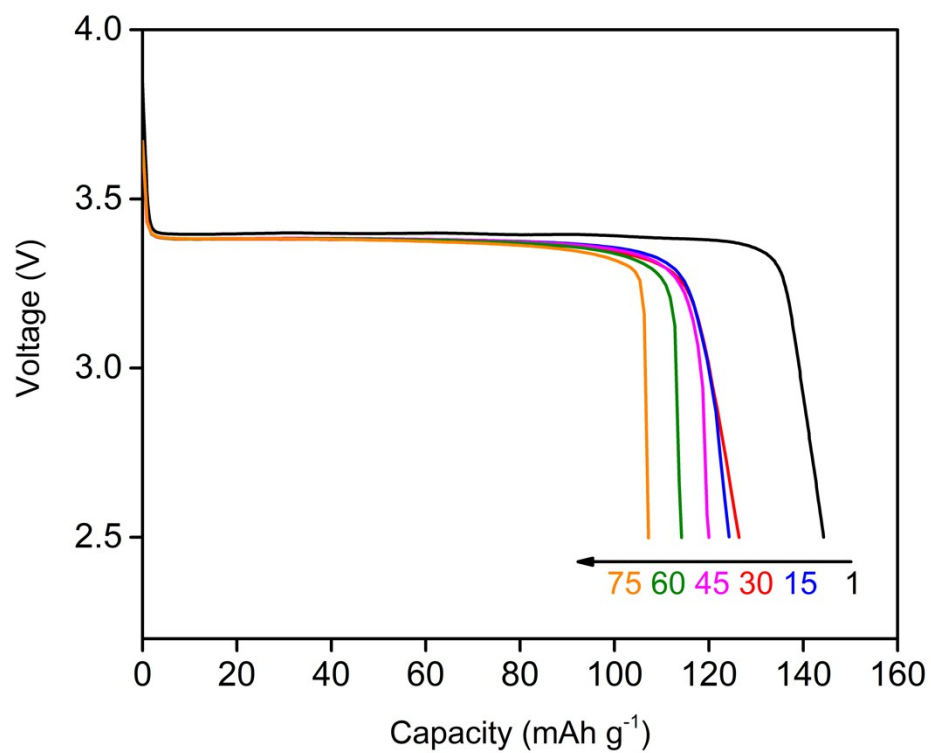


**Figure S20.** Discharge curves of a Li | LFP full cell with DME+DOL+TEGDME electrolyte at different cycles.

## References:

- [1] a) G. Kresse, J. Hafner, *Phys. Rev. B* **1993**, *47*, 558-561; b) G. Kresse, J. Hafner, *Phys. Rev. B* **1994**, *49*, 14251-14269; c) G. Kresse, J. Furthmüller, *Comp. Mater. Sci.* **1996**, *6*, 15-50; d) G. Kresse, J. Furthmüller, *Phys. Rev. B* **1996**, *54*, 11169-11186.
- [2] a) P. E. Blöchl, *Phys. Rev. B* **1994**, *50*, 17953-17979; b) G. Kresse, D. Joubert, *Phys. Rev. B* **1999**, *59*, 1758-1775.
- [3] a) J. P. Perdew, K. Burke, M. Ernzerhof, *Phys. Rev. Lett.* **1996**, *77*, 3865-3868;  
b) J. P. Perdew, K. Burke, M. Ernzerhof, *Phys. Rev. Lett.* **1997**, *78*, 1396-1396.
- [4] K. Momma, F. Izumi, *J. Appl. Crystallogr.* **2011**, *44*, 1272-1276.